High Dynamic Range Photon Counting Imagers Using Nano-Engineered Microchannel Plates

C. D. Ertley, O. H. W. Siegmund, J. Hull, A. Tremsin, A. O'Mahony, C. A. Craven, M. J. Minot

***Abstract*–This work focuses on the development of novel nano-engineered microchannel plates (MCPs) to enhance a new generation of NUV-visible light photon counting detectors that have a wide range of applications in LIDAR, 3D topographic imaging, high-speed photography, bio-medial fluorescence microscopy and astronomical imaging. The MCPs are borosilicate glass micro-capillary arrays functionalized using atomic layer deposition (ALD). MCP's manufactured in this way have many advantageous properties, including the ability to withstand high processing temperatures, high secondary electron yield, and low outgassing. This scheme has the ability to support higher global photon count rates while greatly reducing the deterioration of photocathode efficiency and detector gain. Opaque photocathodes have been deposited onto these nano-engineered borosilicate MCPs and several sealed tube devices have been constructed. Here we report on the progress of this effort, including performance and lifetime characteristics from the sealed tubes and MCPs, and results from the deposition of opaque photocathodes onto nano-engineered MCPs.**

I. Introduction

Microchannel plate (MCP) photon counting, event timing, imaging detectors have found wide use in astronomical [1][2], remote sensing [3], and biological imaging [4] applications. Combining high spatial resolution (~10-100 μm in formats of several cm) with very high time resolution (sub-ns) can enhance the performance of such detectors in dynamic environments, in particular by allowing complete and noiseless correction of sensor and/or target motion without a priori knowledge of that motion. Since there is no read noise in a true photon counter and dark noise is very small, all photon events contain information and the rate at which information is collected is limited only by the total photon detection rate. But the limited dynamic range (up to ~1 MHz detected photon rate over an entire XDL sensor) limits the total information that can be acquired. Next-generation crossed strip MCP sensors are currently being developed [5][6], to give count rate improvements of ~10 times this rate. Specialized pixelized CMOS readout anodes also exist that push event rates up to 100 MHz, though currently sacrificing nanosecond timing [7][8]. For many applications, to visualize brighter scenes or fast transient behavior, or to take advantage of higher throughput optics, the ideal sensor would combine the desirable attributes of high spatial and time resolution for each detected photon with event rates of 100 MHz or more. This work uses a new class of borosilicate substrate nano-engineered surface MCPs, which have significant advantages over their lead-glass counterparts to enhance the lifetime and performance of sealed tube imaging-timing photo-detectors.

Manuscript received November 23, 2015. This work was supported by NASA grants NNG11AD54G & NNX14AD34G and DOE grant 005099.

C. D. Ertley is with the Space Sciences Laboratory, University of California – Berkeley, Berkeley, CA 94720 USA (telephone: 510-664-4699, e-mail: camden.ertley@ssl.berkeley.edu).

O. H. W. Siegmund is with the Space Sciences Laboratory, University of California – Berkeley, Berkeley, CA 94720 USA (telephone: 510-642-0895, e-mail: ossy@ssl.berkeley.edu).

A. Tremsin is with the University of California-Berkeley Space Sciences Laboratory, Berkeley, CA, 94720 (telephone: 510-642-4554, email: ast@ssl.berkeley.edu)

J. Hull is with the University of California-Berkeley Space Sciences Laboratory, Berkeley, CA, 94720 (telephone: 510-643-9730, email: jhull@ssl.berkeley.edu)

A. O'Mahony is with Incom, Inc., Charlton, MA 01507 (telephone: 508-909-2248, email: aom@incomusa.com)

C. A. Craven is with Incom, Inc., Charlton, MA 01507 (telephone: 508-909-2277, email: cac@incomusa.com)

M. J. Minot is with Incom, Inc., Charlton, MA 01507 (telephone: 508-909-2369, email: mjm@incomusa.com)

II. ALD MCPs

A program is underway to develop a new class of MCPs that have been constructed using atomic layer deposition (ALD) on borosilicate glass microcapillary arrays. The substrates are being fabricated using inexpensive borosilicate tubes, which are drawn and fused into microcapillary arrays. The substrates are then functionalized with a resistive layer and an emissive layer using the ALD process [9]. This process does not require the removal of a core glass from the microcapillary array or the activation of the MCP by hydrogen reduction, steps that are required in conventional MCP construction. A contact electrode can be applied to the top and bottom surfaces after the functionalization is complete. Fig.1 shows a diagram of the cross section of an ALD MCP.

The ALD MCP manufacturing process discussed here allows for the operation parameters, such as resistance, to be tailored to the specific application. The borosilicate substrates are very robust and can withstand high temperatures before softening (>700 ˚C) allowing for many high temperature enhancement procedures to be considered. The substrates can also be made in large areas (currently testing 200 × 200 mm^2 MCPs) and large open area ratios (up to 83%). Other advantages of the borosilicate substrate include low radioactive content (low intrinsic background) and low outgassing (longer life and shorter processing times) [10][11]. The functionalization is decoupled from the substrate opening the door for many new resistive and high secondary emissive materials.

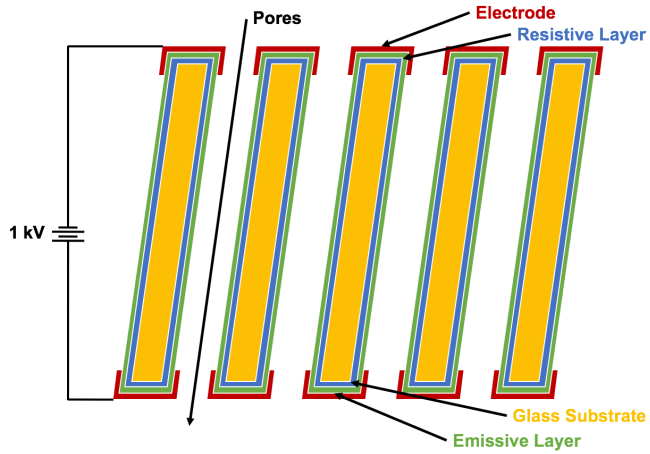

Fig. 1: Borosilicate glass substrates are functionalized with atomic layer deposition. Resistances can be tailored to suit the application. Materials with high stable secondary emission can be used since they are decoupled from the substrate.

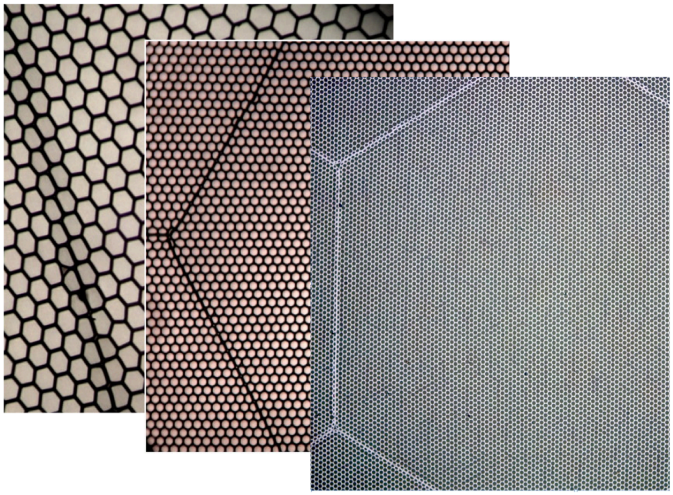

Fig. 2: Photo of 40 µm pore 80%, 20 µm pore 65%, and 10 µm pore 60% open area borosilicate micro-capillary arrays.

High quality borosilicate microcapillary substrates are being produced by Incom, Inc. for use as MCPs (Fig. 2). A second generation borosilicate glass is being used to produce substrates with pore sizes ranging from 10 µm – 40 µm, bias angles of 8º and 13º, and pore length to diameter ratios of 80:1, 60:1, and 40:1. Substrates with open area fractions from 55% to 83% in several sizes ranging from 25 mm circular to 200 mm square have been fabricated. Functionalization of the substrates has been happening at Argonne National Laboratory and will soon be done at Incom Inc. The functionalized MCPs are sent to the University of California, Berkeley Space Science Laboratory for testing. Borosilicate MCPs with secondary emissive layers of Al_2O_3 and MgO and resistances from 5 MΩ to > 1 GΩ have been produced and tested.

III. 33 MM ALD MCPS

Results from new batch of 33 mm MCPs with the 2nd generation 20 µm pore borosilicate substrates and Al_2O_3 and MgO emissive layers are reported here. The new MCPs show very consistent gain curves (Fig. 3) and have higher gain (10^3 at 800v) than previous samples. Most implementations of MCPs require some form of preconditioning [12]. Vacuum baking and scrubbing are done to optimize the stability of sealed tube devices. Gain stability is especially important in open face detectors, where re-exposure to atmospheric pressure is likely. The gain of these MCPs decreased slightly during a vacuum bake, however the imaging and gain maps remained consistent and uniform (Fig 4).

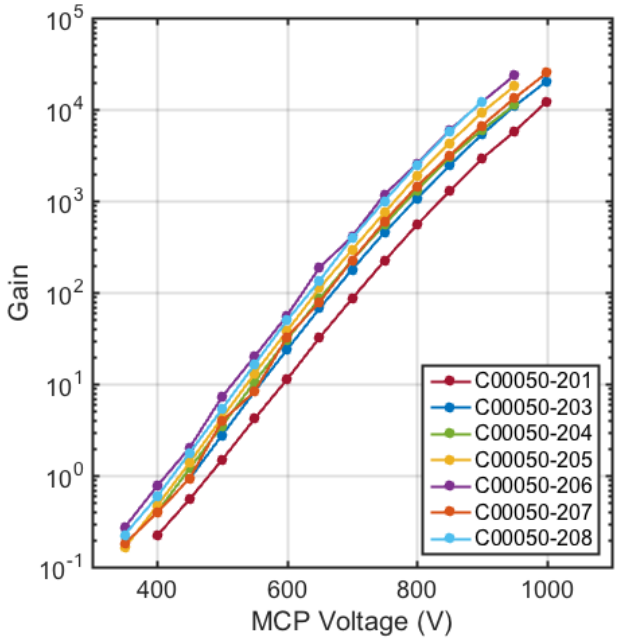

Fig. 3: Gain for 33 mm ALD MCPs on 2nd generation glass with Al_2O_3 emissive layers, 20 µm pores, 60:1 l/d, 8° bias.

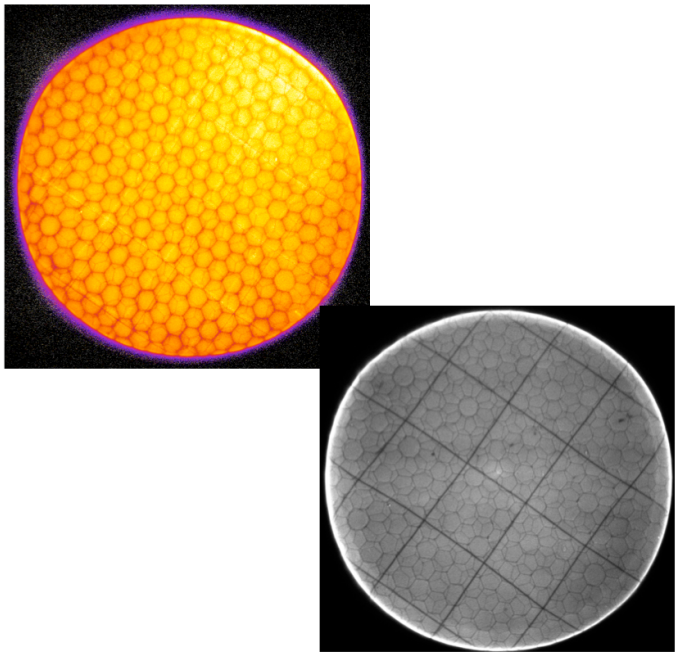

Fig. 4: Gain map & intensity image (showing QE grid) for 2nd generation 33 mm ALD MCPs. 20 µm pores, 60:1 l/d, 8° bias.

The background event rate measured for the MCP samples is as low as ~0.07 events cm^{-2} sec^{-1} (Fig. 5). Standard MCPs in

a similar configuration have background rates on the order of ~0.25 events cm^{-2} sec^{-1}. This rate is dominated by the ^{40}K decay in the MCP glass. Borosilicate glass MCPs have a reduced level of ^{40}K, which is proportional to the reduction in observed background rates. Muon detection accounts for ~0.02 events cm^{-2} sec^{-1} of the background [11].

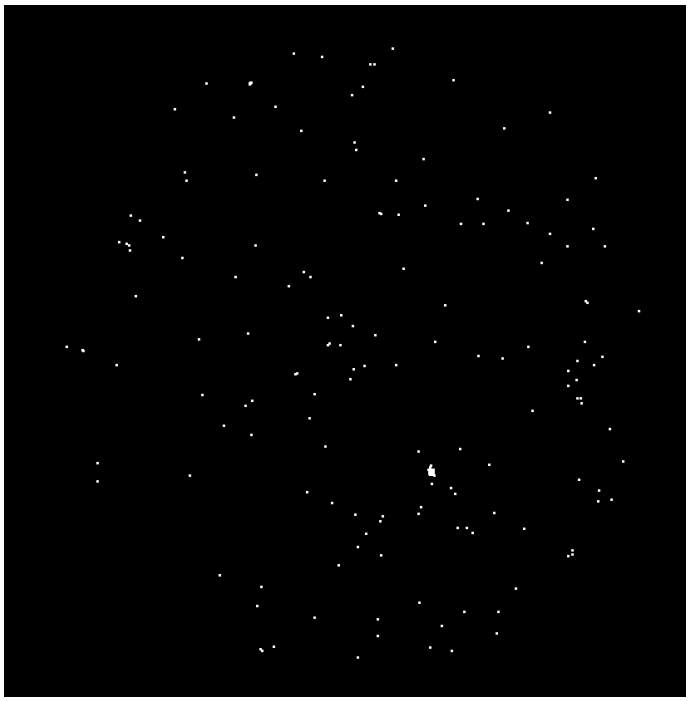

Fig. 5: 500 sec MCP background for 74% open area ALD 33 mm MCPs with MgO emissive layer, 20 µm pores, 60:1 l/d, 8° bias. Rate is ~0.07 events sec^{-1} cm^{-2} except for one "warm" spot.

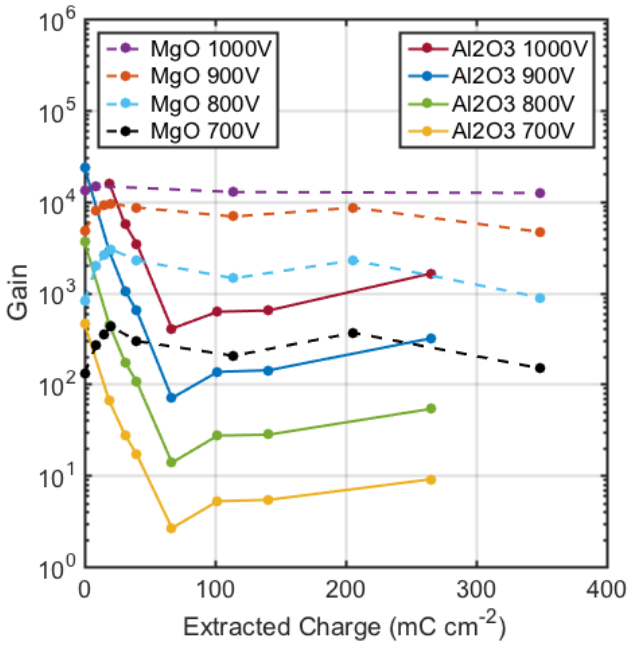

Fig. 6: Comparison of 33 mm ALD MgO and Al_2O_3 MCP with 2nd gen glass. Gain during electron scrubbing.

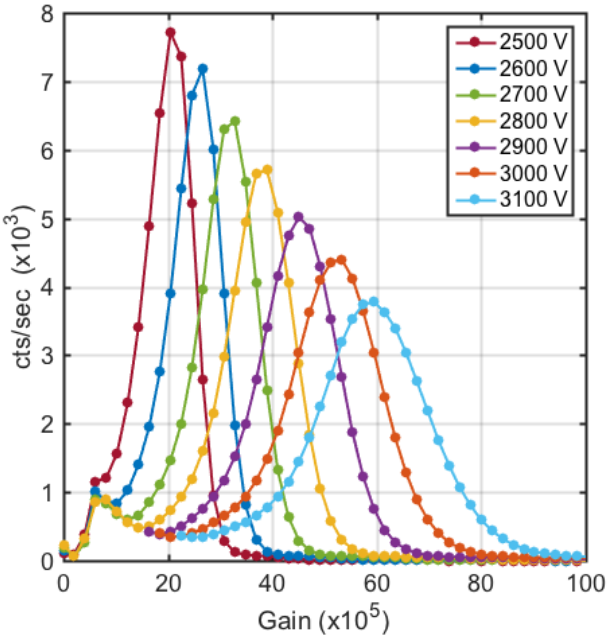

Fig. 7: Tight pulse amplitude distributions at low gain, 3 MCP stack with 20 µm pores, 60:1 l/d, 8° bias [14].

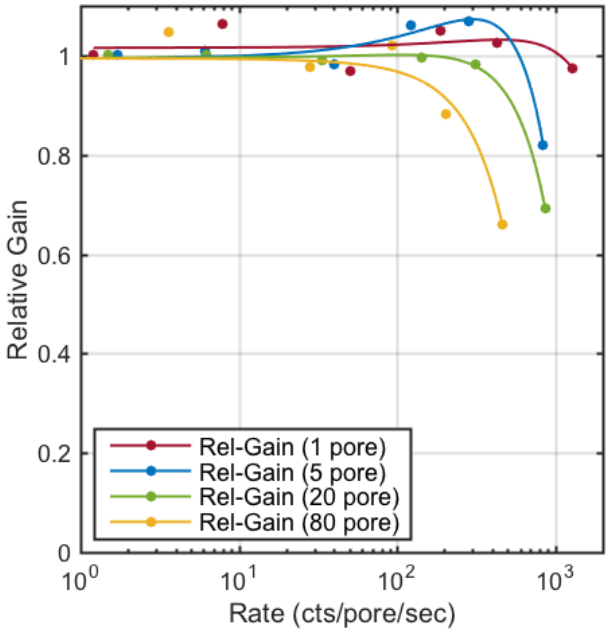

Fig. 8: Gain droop for MCP pair (8 MΩ each) at high gain (5×10^6), high rates in small spots. Rates of ~10^3 events $pore^{-1}$ sec^{-1} before onset.

For borosilicate ALD MCPs, the secondary emissive layer is the most important factor for the behavior of the MCP performance stability. The two materials generally used are Al_2O_3 or MgO emissive layers. 2nd generation ALD MCPs coated with Al_2O_3 tend to show decreases (~factor of >10) in gain during burn-in and stabilize after ~0.05 C cm^{-2}. Conversely the MgO coated MCPs show an initial increase in gain by a factor of ~5 during burn-in and seem to stabilize at 0.1 to 0.2 C cm^{-2} (Fig. 6). A potential explanation for this is the difference in surface bonding between the two species. Jokela et al. [13] found the secondary electron yield for MgO

surfaces increases after the removal of surface carbon, while Al_2O_3 yield was found to decrease. The gain is dramatically affected by small changes in the secondary electron yield due to multiple wall interaction during the amplification process.

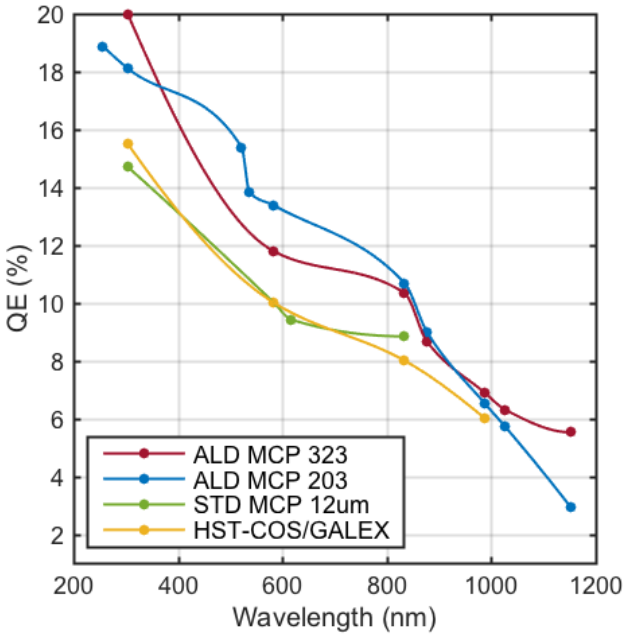

Fig. 9: MCP QE for 74% open area ALD MCPs with Al_2O_3 emissive layer, 20 µm pores, 60:1 l/d, 8° bias, vs. standard MCPs.

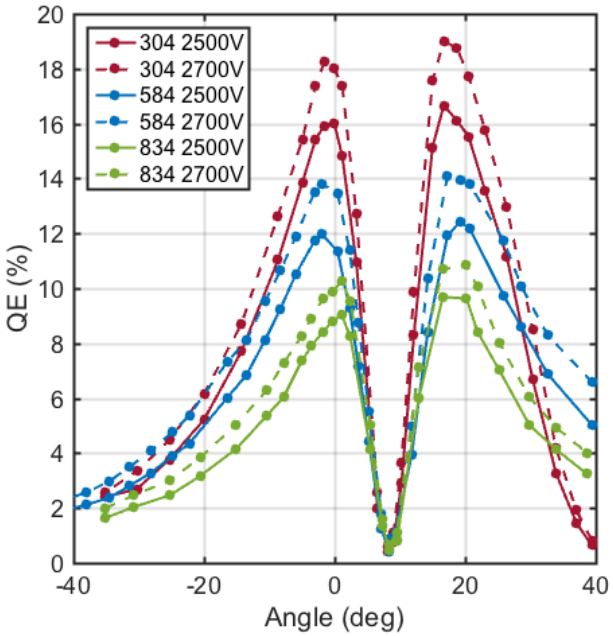

Fig. 10: Angular dependence of QE for 74% open area ALD MCPs with Al_2O_3 emissive layer, 20 µm pores, 60:1 l/d, 8° bias, at two bias potentials.

ALD MCPs are excellent candidates for low gain – high rate devices. Testing of a three plate stack of 33 mm 20 µm Al_2O_3 and MgO coated borosilicate substrate MCPs in a "Z" configuration shows these MCPs have extremely narrow pulse height distributions at low gain (Fig. 7). Low resistance plates have been shown to have high rate gain stability, with supportable rates up to ~40×10^3 events sec^{-1} in a 100 µm spot (Fig. 8).

The quantum detection efficiency (QE) of MCPs with no photocathode can be a good indicator of MCP performance. Two batches of ALD MCPs tested have shown consistently higher QE measurements compared to historical (HST-COS [1]) and recent conventional MCP (standard 12 µm MCP) efficiencies. This is likely partially due to the larger open area ratio of the ALD substrates and the effect of the higher secondary emission coefficients. These measurements indicate that new substrates with larger open areas will have increased electron/ion [15] and photon detection efficiencies. The angular dependence of the QE shows the peak efficiency at ±8° from the bias direction (Fig. 10). The minimum corresponds to the light source being incident normal to the pore bias. Many of the photons at this angle interact deep within the pore and therefore do not have enough gain to produce a signal above the threshold.

IV. 53MM ALD MCPS

We have made extensive measurements of the 10 µm pore 53 × 53 mm^2 ALD MCPs. The gain of these Al_2O_3 coated MCPs and pulse amplitude distributions is comparable to standard MCPs (Fig. 11). Intensity images (Fig. 12) and gain maps (Fig.13) show the latest generation of 53 mm MCPs are very uniform. The next batch (3rd) of 10 µm pore 53 mm MCPs is expected shortly and have much better spatial geometry, which should result in less multifiber modulations.

A pair of 10 µm pore, 53 mm ALD MCPs with 8˚ bias and 60:1 l/d were used for sealed tube, which has been completed [16]. The tube was made with a standard production bialkali photocathode [17] and has a 32 × 32 anode pad readout. Initial data shows the tube is working and has good signal amplification. We are completing firmware algorithms for our test stand to enable us to perform detailed imaging tests and the commencement of lifetests.

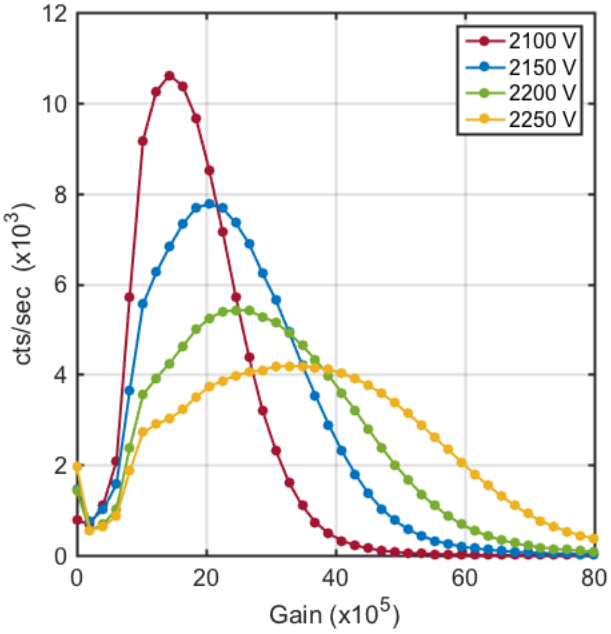

Fig. 11: Pulse height distribution from a stack of two 53 × 53 mm^2, 10 µm pore, 60:1 l/d, 8° bias ALD MCPs.

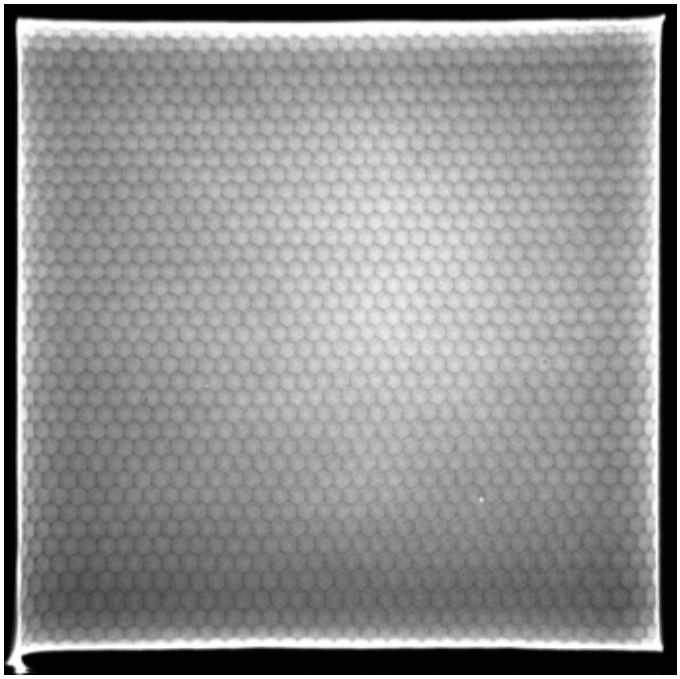

Fig. 12: Intensity image for 53 × 53 mm^2 ALD MCPs with Al_2O_3 emissive layer, 10 µm pores, 60:1 l/d, 8° bias.

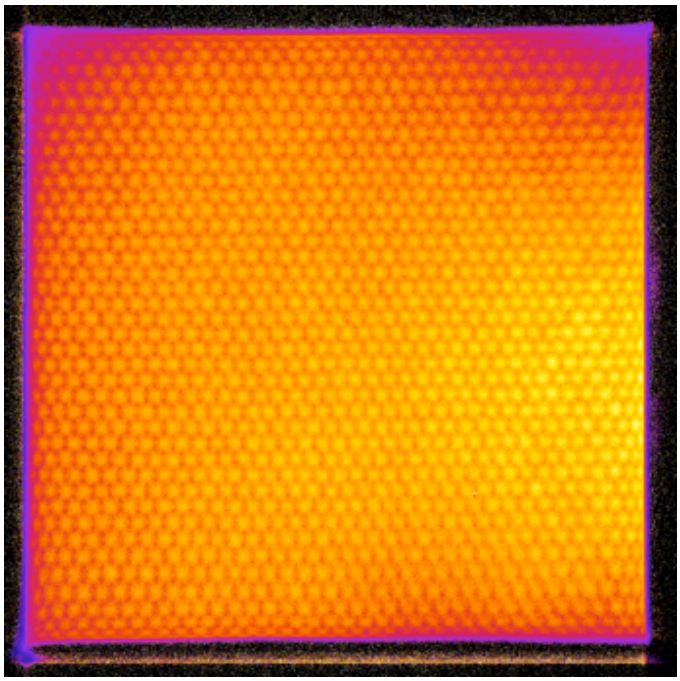

Fig. 13: Gain map for 53 × 53 mm^2 ALD MCPs with Al_2O_3 emissive layer, 10 µm pores, 60:1 l/d, 8° bias. Gain is quite uniform, except for multifiber modulation.

V. Conclusion

ALD MCPs made using borosilicate substrates have been shown to have significant advantages over their lead-glass counterparts, including robust substrates, low outgassing, and high secondary electron yield. As a result, ALD MCPs can support higher global photon count rates while greatly reducing the deterioration of photocathode efficiency and detector gain. Testing second generation ALD MCPs shows high stable gains with very tight pulse amplitude distributions and very low backgrounds (~0.07 events sec^{-1} cm^{-2}). The QE of bare ALD MCPs is constantly better than traditional MCPs implying good performance in sealed tube detectors. These results will improve the next generation of ALD MCPs and the design of future devices.

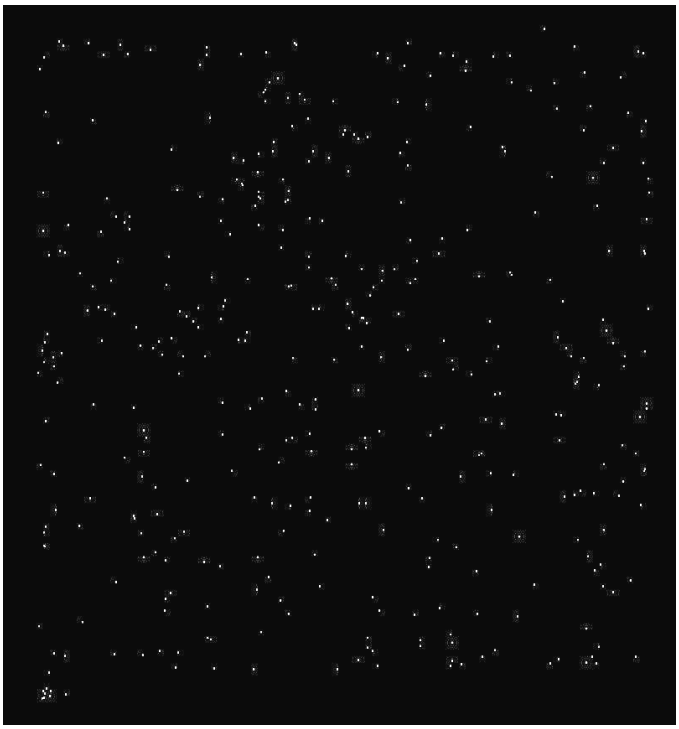

Fig. 14: Background events are very low, a rate of 0.15 events sec^{-1} cm^{-2} for the 53 × 53 mm^2 10 µm pore, 60:1 l/d, 8° bias ALD MCP pair.

Acknowledgements

We wish to thank J. Tedesco and S. Jelinsky for their contributions to this work. We would also like to thank Dr. J. Elam, Dr. R. Wagner and Dr. A. Mane at Argonne National Laboratory, and Prof. H. Frisch at University of Chicago. This work was supported by NASA grants NNG11AD54G & NNX14AD34G and DOE grant 005099.

References

[1] J. Vallerga, J. Zaninovich, B. Welsh, O. H. W. Siegmund, J. McPhate, J. Hull, G. Gaines, and D. Buzasi, "The FUV detector for the cosmic origins spectrograph on the Hubble Space Telescope," Nucl. Instr. Meth. Phys. Res. A, vol. 477, no. 1, pp. 551–555, Jan. 2002.

[2] O. H. W. Siegmund, J. McPhate, A. Tremsin, J. Vallerga, B. Y. Welsh, and J. M. Wheatley, "High time resolution astronomical observations with the Berkeley Visible Image Tube," presented at the AIP Conference Proceedings, 2008, vol. 984, pp. 103–114.

[3] W. Priedhorsky and J. J. Bloch, "Optical detection of rapidly moving objects in space," Appl. Opt., vol. 44, no. 3, pp. 423–433, Jan. 2005.

[4] X. Michalet, R. A. Colyer, G. Scalia, S. Weiss, O. H. W. Siegmund, A. Tremsin, J. Vallerga, F. Villa, F. Guerrieri, I. Rech, A. Gulinatti, S. Tisa, F. Zappa, M. Ghioni, and S. Cova, "New photon-counting detectors for single-molecule fluorescence spectroscopy and imaging," presented at the Proceedings of the SPIE, 2011, vol. 8033, pp. 803316–803316–12.

[5] O. H. W. Siegmund, J. Vallerga, A. Tremsin, L. C. Stonehill, R. Shirey, M. W. Rabin, and D. C. Thompson, "Cross strip microchannel plate imaging photon counters with high time resolution," presented at the Proceedings of SPIE, 2010, vol. 7681, pp. 768109–768109–11.

[6] L. C. Stonehill, J. S. Salacka, I. J. Owens, M. W. Rabin, R. Shirey, D. C. Thompson, O. H. W. Siegmund, A. Tremsin, and J. Vallerga, “Cross-strip anodes for high-rate single-photon imaging,” IEEE Nucl Sci Conf R, pp. 1417–1421, 2009.

[7] J. Vallerga, J. McPhate, A. Tremsin, and O. H. W. Siegmund, “High-resolution UV, alpha and neutron imaging with the Timepix CMOS readout,” Nucl. Instr. Meth. Phys. Res. A, vol. 591, no. 1, pp. 151–154, Jun. 2008.

[8] J. Vallerga, J. McPhate, A. Tremsin, and O. H. W. Siegmund, “Optically sensitive MCP image tube with a Medipix2 ASIC readout,” Proc. SPIE, vol. 7021, pp. 702115–702115–11, Jul. 2008.

[9] Ritala, M., Leskelä, M.. “Atomic layer epitaxy - a valuable tool for nanotechnology?,” Nanotechnology 10:1, 19 (1999)

[10] Siegmund, O.H.W., McPhate, J.B., Jelinsky, S.R., Vallerga, J.V., Tremsin, A.S., Hemphill, R., Frisch, H.J., Wagner, R.G., Elam, J., Mane, A., "Large area microchannel plate imaging event counting detectors with sub-nanosecond timing," IEEE. Trans. Nucl. Sci. 60(2), 923-931 (2013)

[11] Siegmund, O.H.W., Gummin, M.A., Stock, J., Marsh, D., “Microchannel plate imaging detectors for the ultraviolet,” Proc. of an ESA Symposium on Photon Detectors for Space Instrumentation SP-356, (1992).

[12] Siegmund, O.H.W. "Preconditioning Of MCP Stacks," Proc. SPIE, 1072, pp.111–118, (1989)

[13] Jokela, S. J., Veryovkin, I. V., Zinovev, A. V., Elam, J. W., Mane, A. U., Peng, Q., & Insepov, Z., "Secondary Electron Yield of Emissive Materials for Large-Area Micro-Channel Plate Detectors: Surface Composition and Film Thickness Dependencies," Physics Procedia, 37, pp. 740–747, (2012).

[14] Ertley, C., Siegmund, O. H. W., Schwarz, J., Mane, A. U., Minot, M. J., O'Mahony, A., Craven, C. A., Popecki, M., “Characterization of borosilicate microchannel plates functionalized by atomic layer deposition,” Proc. SPIE, vol. 9601, pp. 96010S-96010S-10, (2015).

[15] Siegmund, O.H.W., Samson, J. & Ederer, D.L.,"Methods of vacuum ultraviolet physics," (1998).

[16] Siegmund, O. H. W., Ertley, C., and Vallerga, J., “High Speed Large Format Photon Counting Microchannel Plate Imaging Sensors,” Proceedings of the Advanced Maui Optical and Space Surveillance Technologies Conference, held in Wailea, Maui, Hawaii, September 15-18, 2014, Ed.: S. Ryan, The Maui Economic Development Board, id.94, vol. 1, p. 94, (2015).

[17] Siegmund, O. H. W., Vallerga, J., Tremsin, A., Hull, J., Elam, J., and Mane, A., “Optical and UV Sensing Sealed Tube Microchannel Plate Imaging Detectors with High Time Resolution,” presented at the Proceedings of the Advanced Maui Optical and Space Surveillance Technologies Conference, (2014).